Chapter 6

Nanoplasmonic Biosensor Using Localized Surface Plasmon Resonance Spectroscopy for Biochemical Detection

Diming Zhang, Qian Zhang, Yanli Lu, Yao Yao, Shuang Li, and Qingjun Liu

Abstract

Localized surface plasmon resonance (LSPR) associated with metal nanostructures has developed into a highly useful sensor technique. Optical LSPR spectroscopy of nanostructures often shows sharp absorption and scattering peaks, which can be used to probe several bio-molecular interactions. Here, we report nanoplasmonic biosensors using LSPR on nanocup arrays (nanoCA) to recognize bio-molecular binding for biochemical detection. These sensors can be modified to quantify binding of small molecules to proteins for odorant and explosive detections. Electrochemical LSPR biosensors can also be designed by coupling electrochemistry and LSPR spectroscopy measurements. Multiple sensing information can be obtained and electrochemical LSPR property can be investigated for biosensors. In some applications, the electrochemical LSPR biosensor can be used to quantify immunoreactions and enzymatic activity. The biosensors exhibit better performance than those of conventional optical LSPR measurements. With multi-transducers, the nanoplasmonic biosensor can provide a promising approach for bio-detection in environmental monitoring, healthcare diagnostics, and food quality control.

Key words Localized surface plasmon resonance (LSPR), Nanocup arrays (nanoCA), Electrochemistry, Biosensor, BSA (bull serum albumin), Thrombin

1 Introduction

Optical detection is particularly a promising method because it allows remote transduction without any physical connection between excitation sources and detecting elements. In recent years, several nanostructured sensors such as photonic crystal, whispering gallery mode (WGM), and surface plasmon resonance (SPR) were increasingly being employed by optical spectroscopy for DNA detection, antigen-antibody recognition, immunoassays probing, and pathogen identification [1–3]. These sensors can respond to target molecules at low concentrations by observing shifts in resonance wavelength before and after conjugation of biomolecules to the sensor surfaces. A common drawback, however, is that optical

Avraham Rasooly and Ben Prickril (eds.), *Biosensors and Biodetection: Methods and Protocols Volume 1: Optical-Based Detectors*, Methods in Molecular Biology, vol. 1571, DOI 10.1007/978-1-4939-6848-0_6,

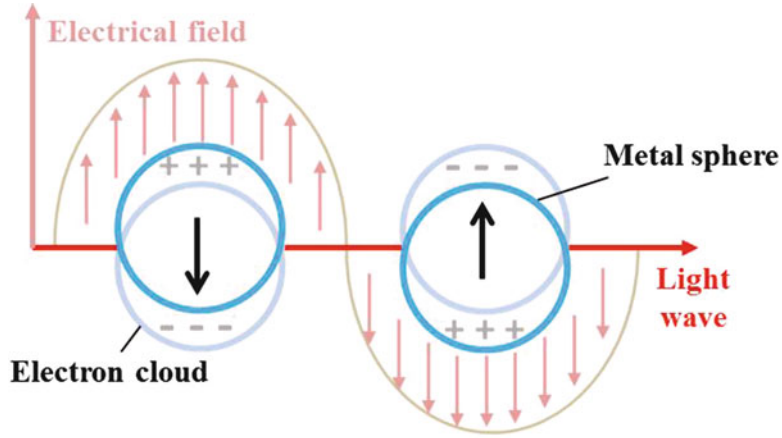

Fig. 1 Schematic of localized surface plasmon resonance (LSPR), where the free conduction electrons in the metal sphere are driven into oscillation due to coupling with incident light

biosensors, such as SPR and WGM, often required a complex system. They should fabricate devices that ensure precise alignment of light coupling to bio-detection volume and generate the desired optical phenomena.

Metal nanostructures were recently reported to modulate localized surface plasmon resonance (LSPR) spectroscopy for probing biomolecular interactions [4–6]. LSPR was often induced by incident light when it interacted with noble metal nanostructures, such as gold nanoparticles, that had smaller sizes than the wavelength of the incident light (Fig. 1). The light can be coupled in direct perpendicular transmission between incident light and spectrometer to obtain LSPR wavelength shifts without complex optical coupling [7–9]. Thus, it can be measured by a robust optical sensing platform minimizing the alignment requirement. However, sizes and positions of single nanostructures such as colloid nanoparticles were always random and difficult to control over a large area. Thus, the wavelength shift may be different for the same analyte because nanoparticles of different sizes gave rise to different optical spectroscopy as biosensors [8]. To generate stable LSPR spectroscopy, periodic nanostructure arrays such as nanohole arrays, nanorod arrays, and nanocone arrays can be fabricated by several nanoelectromechanical systems including electron beam lithography and focused ion beam milling for biosensing [9, 10]. These nanostructures were often fabricated by scanning beam lithographies, such as electron beam lithography (EBL) and focused ion beam (FIB) lithography. Thus, compared to nanoparticles from chemical synthesis, these nanostructure arrays with their more precise sizes and positions provide a promising approach to producing repeatable and stable LSPR spectroscopy for biological

and chemical detection. Other detection techniques such as electrochemistry can also be combined with LSPR spectroscopy of nanostructures while providing unique advantages in sensitivity and selectivity. For instance, voltammetry can be used to modulate electrochemical reactions on nanostructures and provide additional selectivity to LSPR monitoring of α-synuclein–small molecule interactions [11].

Nanoimprint lithography is a method of fabricating nanometer scale patterns, and offers advantages including low cost, high throughput, and high resolution. It often creates nanostructure patterns by molding and curing of monomer or polymer resist on nanostructured template, while adhesion between the resist and the template is controlled to allow proper release. Nanoimprint lithography is currently used to fabricate devices for electrical, optical, photonic, and biological applications [12, 13]. In our work, nanocup arrays (nanoCA) were fabricated by nanoimprint and deposited with nanoparticles to modulate a stable LSPR spectroscopy for biosensor applications [14–16]. Nanoplasmonic biosensors using nanoCAs can be employed to monitor small molecule binding to proteins such as odorant binding proteins (OBPs) and peptides, and for odorant and explosive detection. The electrochemical detection technique can also be coupled with LSPR spectroscopy to design an electrochemical LSPR biosensor. This provides multiple sensing information for biosensor applications. The electrochemical LSPR sensor can also be used to quantify immunoreactions and enzymatic activity with demonstrably higher sensitivity.

2 Materials

2.1 Optical and Electrochemical Measurement System

1. Halogen cold light source (DT-MINI-2, Ocean Optics Inc., Dunedin, Florida, USA).
2. Spectrophotometer (USB2000+, Ocean Optics Inc., Dunedin, Florida, USA).
3. Three fiber bundles (QP230-0.25-XSR, Ocean Optics Inc., Dunedin, Florida, USA).
4. Optical fiber attenuator (FVA-ADP-UV, Ocean Optics Inc., Dunedin, Florida, USA).
5. Collimating lens (F230APC-633, Thorlabs Inc., Newton, New Jersey, USA).
6. Absorb sample pool (SPL-CUV-ABS, Pulei Inc., Hangzhou, China).
7. Multi-mode microplate reader (SpectraMax Paradigm, Molecular Devices Co., United Sates).
8. Electrochemical workstation (CHI 660E, CH Instruments, Texas, USA).

9. Ag/AgCl reference electrode (CHI 111, CH Instruments, Texas, USA).
10. Pt counter electrode (CHI 102, CH Instruments, Texas, USA).

2.2 Acquisition and Immobilization of Proteins

1. Phosphate buffer saline (PBS) (*see* **Note 1**).
2. 2-(morpholino)ethanesulfonic acid (MES) buffer (*see* **Note 2**).
3. 1-ethyl-3-(3-dimethylaminopropyl) carbodiimide (EDC) solution (*see* **Note 3**).
4. *N*-hydroxy-succinimide (NHS) solution (*see* **Note 4**).
5. Carboxy-poly(ethylene)-thiol (HOOC-PEG-SH, 2 kDa, Sigma- Aldrich, USA) (*see* **Note 5**).
6. Recombinant expressed plasmid pET-Acer-ASP2 (from Center of Analysis & Measurement, Zhejiang University) (*see* **Note 6**).
7. *E. coli* BL21 (DE3) (from Center of Analysis & Measurement, Zhejiang University).
8. *Bam*H I endonuclease (TaKaR Co., Dalian, China).
9. *Hind* III endonuclease (TaKaR Co., Dalian, China).
10. Isopropyl-β-D-thiogalactopyranoside (Aladdin, Shanghai, China).
11. OBPs, Acer-ASP2.
12. TNT-specific peptides (*see* **Note 7**).

2.3 Fabrication of nanoCA Device

1. UV light-curing flood lamp system (EC-Series, Dymax, USA).
2. E-beam evaporation system (FC/BJD2000, Temescal, USA).
3. Scanning electron microscope (SEM, XL30-ESEM, Philips, Netherlands).
4. Nanocone quartz template fabricated by e-beam lithography.
5. UV curable polymer (NIL-UV-Si, GuangDuo Nano Ltd., Suzhou, China).
6. Dimethyl dichlorosilane (CP, Aladdin, Shanghai, China).
7. Titanium (>99.99%, Sigma-Aldrich, USA).
8. Gold (99.99%, Sigma-Aldrich, USA).
9. (Poly)ethylene terephthalate (PET) substrate.
10. Teflon roller.
11. Transparent epoxy resin adhesive.

3 Methods

3.1 Fabrication of the nanoCA

The nanoCA device can be fabricated for use in LSPR spectroscopy for monitoring binding events occurring on the surface of the device [14, 17]. The nanostructures were imprinted by nanocone template made on quartz substrate and deposited with gold nanoparticles by following steps, as shown in Fig. 2.

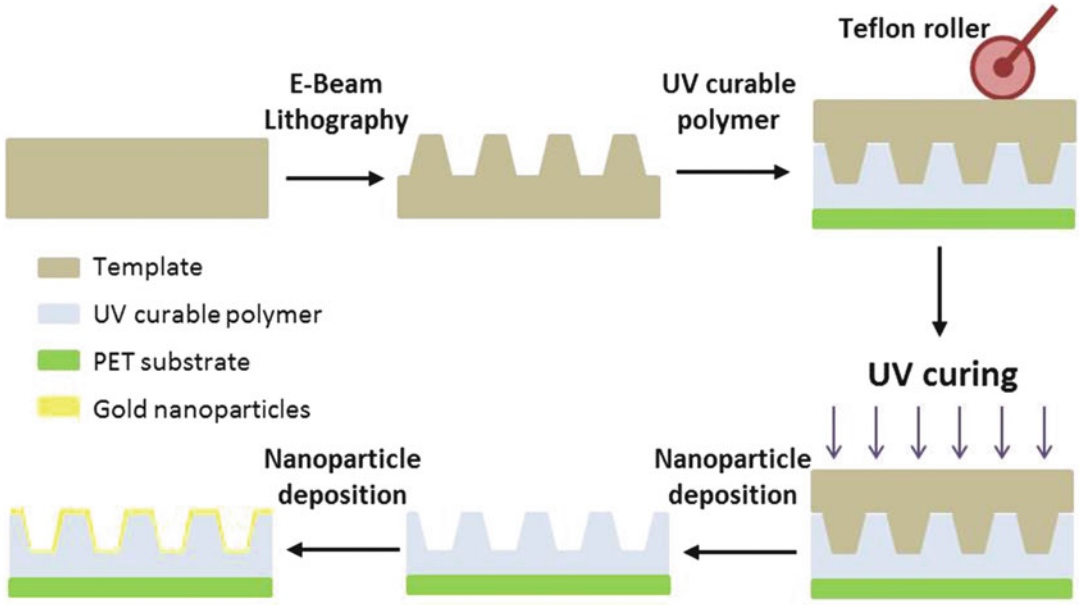

Fig. 2 Flow chart for nanoCA device fabrication by nanoimprint lithography

1. The template had nanocones in arrays, whose height, upper, and base diameter were 300, 200, and 500 nm, respectively. It was passivated with dimethyl dichlorosilane solution for 30 min and then rinsed three times with ethanol and deionized water. This promotes formation of a hydrophobic silane layer on the template, which in turn promotes removal of cured polymer replica with nanocup structures.
2. A 250 μm flexible (Poly)ethylene terephthalate (PET) sheet was used as a supporting substrate, and a Teflon roller was used for evenly distributing the UV curable polymer at the template/PET interface. The depth and opening diameters of the nanocup were 500 and 200 nm respectively, while the diameter of nanoparticles was about 20 nm.
3. To obtain the nanocup array structure, a UV light-curing flood lamp system was used at an average power density of 105 mW/cm^2 to solidify the UV polymer on the template and PET interface. The polymer was cured by UV light for 60 s at room temperature.
4. To deposit gold nanoparticles, 5-nm-thick titanium was deposited first and used as the adhesive layer. Then, gold nanoparticles were deposited on sidewalls and bottom of nanocups. The depositions were both performed with a six pocket e-beam evaporation system. Finally, the nanoCA structure with nanoparticles on sidewalls was successfully fabricated (Fig. 3). Figure 3c shows a scanning electron microscope image of the nanoCA device.

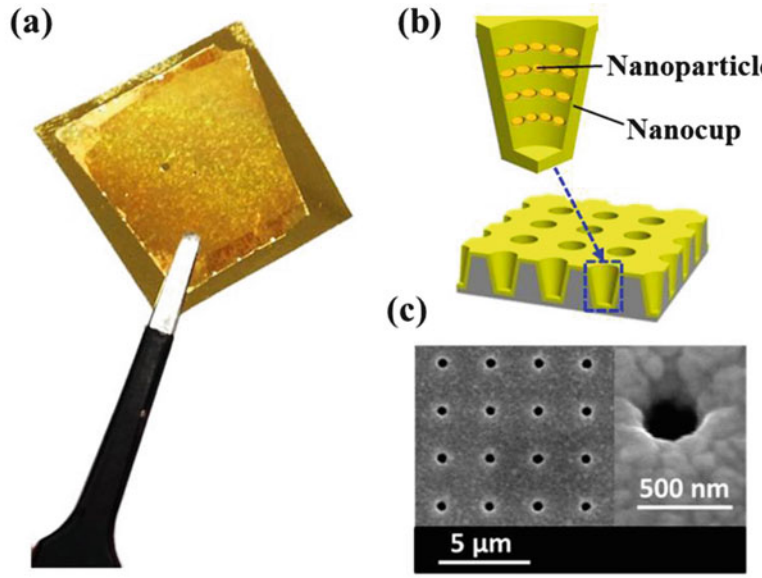

Fig. 3 Fabrication and characterization of nanocup arrays (nanoCA). (**a**) Photograph of nanoCA device in ~ 2 × 2 cm^2. (**b**) Structure of periodic nanocups on nanoCA chip, with Au nanoparticles deposited along the sidewalls. (**c**) SEM image of the cup arrays

3.2 Optical Detection for LSPR Spectroscopy

Periodic nanostructures have prominent optical features such as absorption and transmission peaks in the visible spectrum. These features were elicited by plasmon resonance and can be utilized in optical sensors. The optical detection can be performed using the following steps.

1. As shown in Fig. 3a, the nanoCA chips were first made into small rounds with diameters of 1 cm by hole puncher. Then the rounds can be immobilized on the bottom of wells by transparent epoxy resin adhesive, leaving 6 h for the adhesive to solidify. LSPR spectroscopy was performed using the microplate reader for multi-mode detection in high throughput.
2. A normal transmission model of the microplate reader was applied to measure the spectra of nanoCA. Light was emitted from the light source on the bottom of wells of the plate, delivered through nanoCA chips and received by the spectrometer. The reader detected LSPR spectroscopy in individual wells of the plate. The lamp and spectrograph can move from one well to other wells by a mechanical driver. The scanning range for spectroscopy was set from 300 to 900 nm and the step was fixed at 1 nm.
3. During measurement, 10 μl sample solutions were often added by pipette on the surface of the chip in the wells of the plate. The small volume of the analyte formed a thin liquid layer and reduced interference from the solution itself.

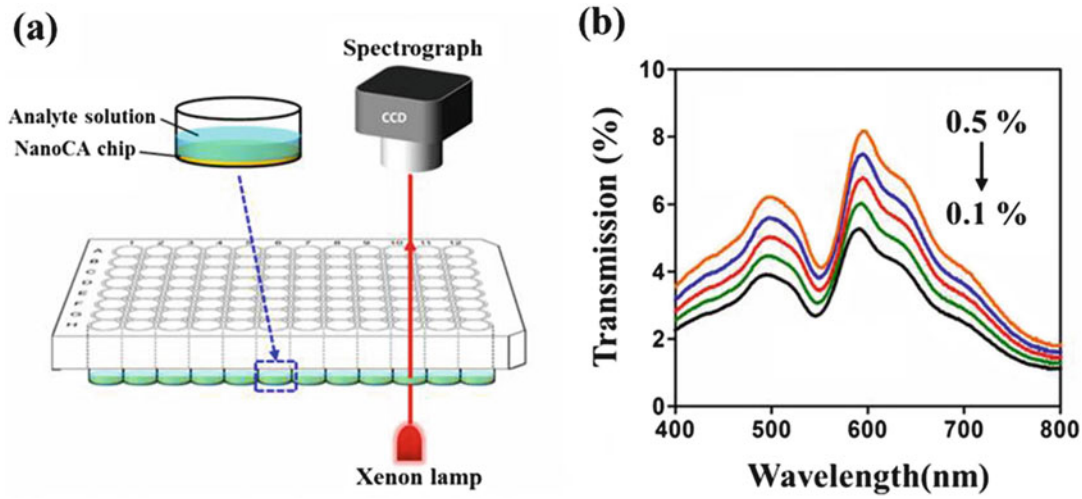

Fig. 4 Nanoplasmonic biosensor system for bio- and chemical detection. (**a**) Schematic diagram of the optical detection using a 96-well plate instrument in transmission mode. (**b**) Transmission spectra of nanoCA in the presence of NaCl at different concentrations (0.1%, 0.2%, 0.3%, 0.4%, and 0.5%). The resonance wavelength shifts with increasing concentration

4. NaCl at different concentrations was employed as increasing refractive index solutions, to determine the refractive-index sensing properties of nanoCA (Fig. 4b). 10 μl NaCl solutions at concentrations of 0.1%, 0.2%, 0.3%, 0.4%, and 0.5% were added by pipette on the surface of the chip. Then, optical detection was performed as described above. The entire transmission spectrum exhibited red shift (shift to right end of the spectrum) with increasing NaCl concentration, indicating the refractive index (RI) sensitivity of nanoCA in LSPR detection. Indeed, transmission peaks around 600 nm were often used as responses of nanoplasmonic sensors. With synergetic LSPR effects of periodical array structure and nanoparticles deposited on the cups, the nanoCA showed a high sensitivity for RI change with ~10^4 nm per refractive index unit (RIU), which was much greater than typical nanoparticle sensors and nanohole sensors based on plasmon resonance [18–20]. Thus, a high-sensitivity LSPR device based on nanoCA is useful as a high-throughput biosensor for monitoring binding of small molecules to proteins.

3.3 Acquisition of Bio-sensitive Material

In sensing property test, the nanoCA device showed a good performance for RIU change on the surface. However, the nanoCA device was only a physical transducer sensitive to refractive index changes, rather than a real sensor with high selectivity to special biochemical analytes. In our work, several olfactory proteins, such as OBPs and peptides, were used to modify nanoCA for bio- and chemical detections.

3.3.1 Expression and Purification of OBPs

Oderant binding proteins (OBPs) are an important class of sensing proteins in biological olfactory systems. OBPs have significant binding affinities to various biochemical molecules. Distinct from membrane proteins or receptors, OBPs are soluble, can be expressed at low cost, purified easily, and maintain bioactivity in vitro [21, 22]. Thus, OBPs are useful as biosensors and can be obtained by the following steps:

- The recombinant OBPs of *Acer-ASP2* were cloned from full-length cDNA of adult worker bees, *Apis cerana cerana*. The recombinant plasmid *pET-Acer-ASP2* was expressed and transformed into *E. coli* BL21 (DE3) competent cells after 450 bp fragments were excised with BamH I and Hind III from the *pGEM-Acer-ASP2* plasmid.
- The cells were grown in Luria–Bertani broth (including 30 μg/ml kanamycin) at 37 °C with 1.5 mM isopropyl-β-D-thiogalactopyranoside to induce expression of the protein. After 5 h at 28 °C, the bacterial cells were harvested and lysed by sonication and centrifuged into crude cell extracts into pellet and supernatant (3 ml, 1740 × g, 10 min).
- The OBP was then collected from the cells. The pellets of crude cell extracts containing recombinant proteins were precipitated in 1.5 M urea in ddH_2O and freeze-dried.
- Finally, the protein was resuspended (500 μg/ml) in phosphate buffered saline (PBS; pH = 7.4) and stored at 4 °C for biosensor experiments. More details can be found in the previous study about expression of the OBPs from honeybee [23].

3.3.2 Synthesis of Peptide

Peptides are short protein fragments composed of a chain of amino acids. Peptides can be designed based on known structures of protein binding sites, synthesized with chemical methods, and purified to obtain specific sequences. They are useful in designing artificial receptors to mimic molecular recognition between proteins and analytes. Thus, peptides are ideal candidates for biosensing materials and for biosensor fabrication.

- TNT-specific peptide was chemically synthesized based on the reported bio-sensitive sequence (WHWQRPLMPVSI) as olfactory protein for TNT [24].
- The peptide (CLVPRGSC) can be cleaved by thrombin, and was synthesized for use in thrombin detection.
- Chemical synthesis of peptides was performed by standard solid-phase peptide synthesis (SPPS) using BOC chemistry, with stepwise addition of protected amino acids to a growing peptide chain. The synthesis work was performed by Genscript company (Nanjing, China). Peptides were stored as freeze-dried powders (*see* **Note 8**).

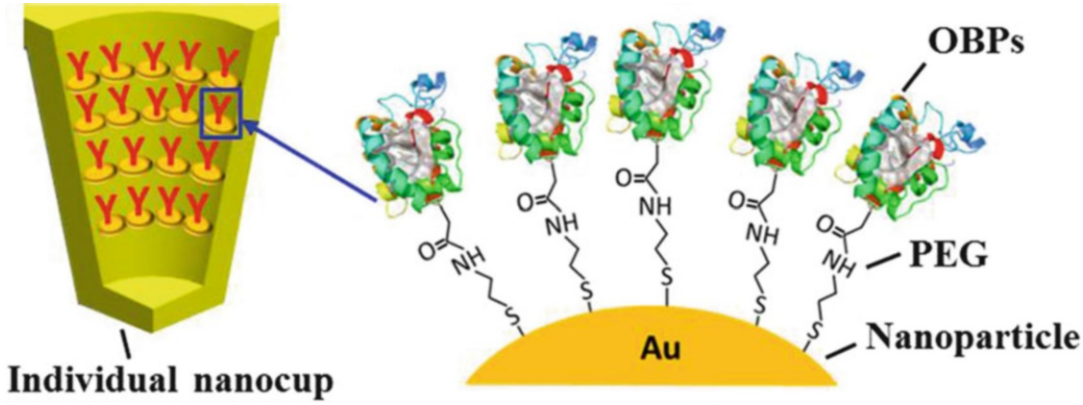

Fig. 5 Self-immobilization of olfactory proteins on sidewalls of nanoCA device

3.4 Self-Immobilization of Proteins

1. The self-immobilization of the proteins on nanoCA was performed by linkage of HOOC-PEG-SH (Fig. 5). The immobilization can be completed by following steps.
2. NanoCA device was first washed with a mixture of 98% H_2SO_4 and 30% H_2O_2 (7:3), and DI water respectively, to remove the organic residues.
3. Subsequently, the nanoCA device was immersed in a petri dish and reacted with 2 ml HOOC-PEG-SH at 1 mg/ml overnight (about 18 h) at room temperature to form Au-S covalent bonding on the surface of the nanoCA device.
4. 2 ml mixing solution of 8 mg/ml EDC and 12 mg/ml NHS in 0.1 M MES buffer (pH = 5, Sigma) was immersed in petri dish for 15 min to activate carboxylate groups of HOOC-PEG-SH after extra HOOC-PEG-SH was washed off with DI water.
5. Finally, the solution was adjusted to pH 8.0 with saturated $NaHCO_3$, added with 1 ml olfactory proteins at 500 μg/ml, and incubated at room temperature for 2 h. The nanoCA was washed with DI water by gentle shaking for 60 s, followed by drying with nitrogen and stored at 4 °C for further experiments (*see* **Notes 8** and **9**).

3.5 Olfactory Protein Modified Sensor Using LSPR Spectroscopy

The interaction between small molecules and olfactory proteins immobilized on nanoCA surface can affect the refractive index in the metal-dielectric interface of nanocup sidewalls and thus give rise to resonance wavelength shift in LSPR spectroscopy. The wavelength shift can then be used to quantify small molecules involved in binding events, and bio-modified nanoCA can be used as a nanoplasmonic biosensor for bio- and chemical detections [15, 16].

3.5.1 LSPR Spectroscopy Analysis for Monitoring of Small Molecule Binding to Protein

The nanoCA can be used as a biosensor by monitoring interactions between small molecules and olfactory proteins. For instance, several chemical molecules can specifically bind into hydrophobic pockets of OBPs immobilized on the nanoCA surface, which can modulate protein conformation and change relative dielectric constants of the bio-coating [15] (Fig. 6a).

– The OBPs were immobilized on the surface of the nanoCA device by self-assembly to obtain OBP-modified nanoCA for monitoring of molecular binding (*see* Subheading 3.4). For odorant measurement one kind of aromatic odorant, β-ionone, was used as a model molecule to test responses of the bio-nanoCA with OBPs. Ten microliter β-ionone solutions at different concentrations ranging from 10 nM to 10 Mm can be added in wells of the 96-well plates by pipette (*see* **Note 10**).

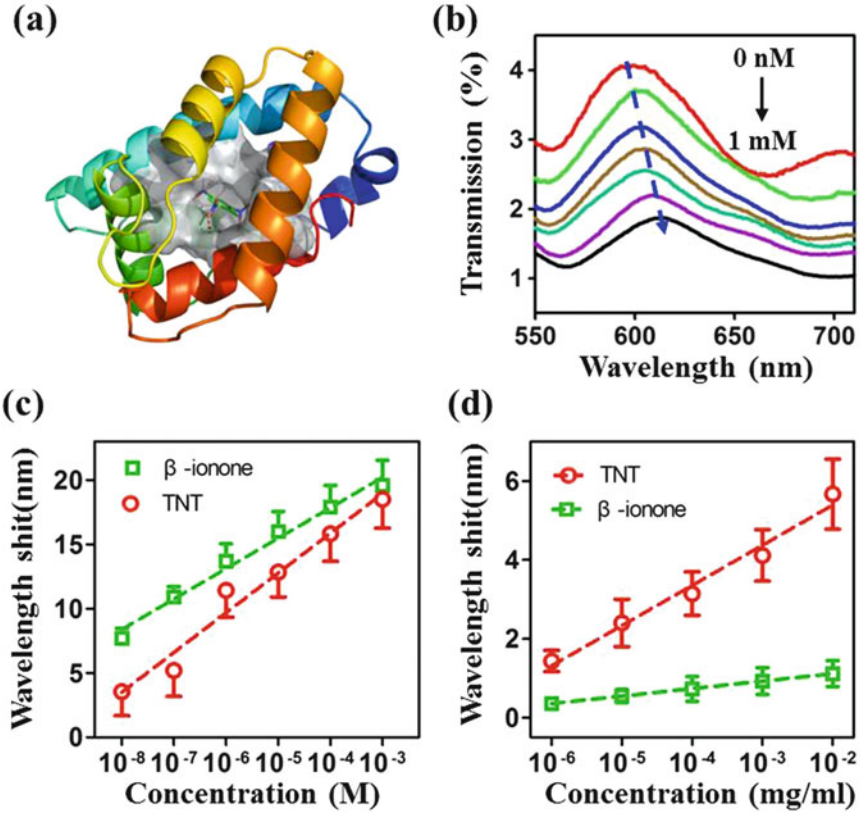

Fig. 6 Bio-nanoCA with olfactory proteins as nanoplasmonic biosensors for odorant and explosive detection. (**a**) Molecular docking of the binding pocket of the OBPs, *Acer-ASP2*. (**b**) Transmission spectrum of OBPs-modified nanoCA for β-ionone. (**c**) Dose-dependent profiles of bio-nanoCA with OBPs in resonance wavelength shift of transmission peak for β-ionone and TNT. (**d**) Dose-dependent profiles of bio-nanoCA with TNT-specific peptide for β-ionone and TNT. (mean ± SD, $n = 15$)

– Optical detection is performed as described above. The transmission spectra of the bio-nanoCA device can be obtained as illustrated in Fig. 6b. Intensity and location of the transmission peak was notably changed by specific binding of β-ionone and OBPs. Transmission intensity change and LSPR wavelength shift can both be calculated statistically with the OBPs-modified devices. As expected, the wavelength shift showed a good linear dose-dependent response for β-ionone at increasing concentrations (Fig. 6c). These results demonstrate that nanoCA can monitor specific binding of β-ionone to OBPs by the resonance wavelength shift in LSPR spectroscopy.

3.5.2 Nanoplasmonic Biosensor for Explosive Detection

Recent studies reported that trained honeybees are able use their sensing proteins to find nitro-explosives, and various OBPs have been used to modify biosensors for explosive detection [25–27]. We have explored the binding of nitro-explosive molecules to the OBPs of *AcerASP2* by the bio-nanoCA.

– Molecular docking of TNT and the OBP was carried out to show affinity of these two molecules. Like β-ionone, TNT molecules can enter protein cavities, interact with amino acid residues, and form a complex with OBPs. This process might elicit OBP conformation changes like those in β-ionone binding, thereby modulating the LSPR on the nanoCA in the optical measurement.
– The OBPs were immobilized on the surface of the nanoCA device by self-assembly to obtain OBP-modified nanoCA for monitoring of molecular binding (*see* Subheading 3.4). Ten microliter TNT solutions at different concentrations can be added in wells of the 96-well plates by pipette. Then, optical detection can be performed as described above (*see* Subheading 3.2). Figure 6c showed responses of the nanoCA with the OBPs to TNT at increasing concentrations. The nanoCA can monitor the binding of TNT molecules to the OBPs. However, the responses were nonlinear in concentration range from 10^{-7} to 10^{-5} M, and the nanoCA cannot distinguish TNT and β-ionone. It indicated that the nanoCA with OBPs was not a good biosensor strategy for explosive detection of TNT.
– The TNT-specific peptide was immobilized on the surface of the nanoCA device by self-assembly to obtain peptide-modified nanoCA for monitoring of molecular binding (*see* Subheading 3.4). Ten microliter TNT solutions at different concentrations can be added in wells of the 96-well plates by pipette. Then, optical detection can be performed as described above (*see* Subheading 3.2). As shown in Fig. 6d, the nanoCA with the peptides was high selective to TNT, while the nanoCA showed no response to β-ionone.

3.6 Electrochemical LSPR Biosensor for Protein Analysis

LSPR is not only influenced by refractive index change on the nanostructure surface, but also by potential and current density on the surface of a metal film [14]. Thus, LSPR sensors can be combined with electrochemistry to implement synchronized electrical and optical responses. The combination of electrochemistry and optical SPR measurement can provide a multitude of information from different signal transductions and provide novel approaches to elucidate detailed processes for electrochemical reactions.

3.6.1 Electrochemical LSPR Measurement

The apparatus for electrochemical LSPR measurement is depicted in Fig. 7a. Optical measurement was performed in transmission mode. The light was emitted from the source below the nanoCA device, delivered through the device, and finally received by a spectrophotometer. The LSPR signal was measured and analyzed by transmission spectroscopy.

– For electrochemical measurements the potentiodynamic electrochemical measurement of cyclic voltammetry (CV) was used to investigate the electrochemistry properties of nanoCA device and the electrochemical modulation to LSPR. The nanoCA device was used as the working electrode, while platinum

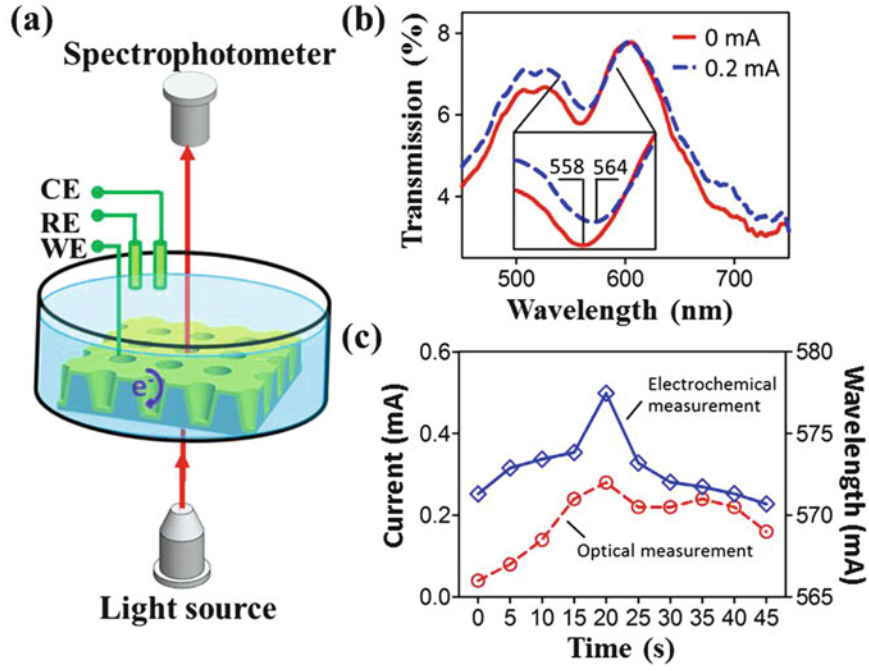

Fig. 7 Electrochemical LSPR spectroscopy measurement. (**a**) Schematic of experimental apparatus for synchronous electrochemical and optical measurement. (**b**) Transmission LSPR spectroscopy of nanoCA with different surface currents. (**c**) Synchronous measurement of LSPR and electrochemistry in CV scanning

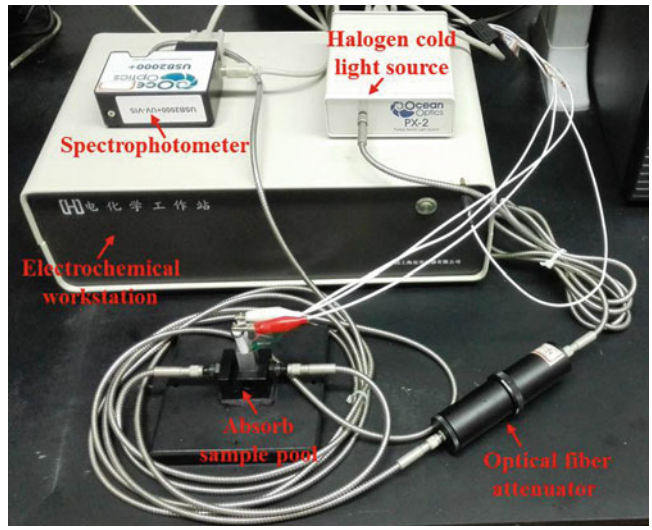

Fig. 8 Photograph of the electrochemical LSPR measurement apparatus

electrode and Ag/AgCl electrodes were used as counter electrode and reference electrodes, respectively.

– In the synchronous measurement, the range of the transmission spectrum was from 300 to 1000 nm with a step of 0.5 nm. The transmission spectrum can be recorded when the surface of nanoCA had RI change and electrochemical current (Fig. 7b). The electrochemical reactions were measured using an electrochemical workstation in a standard three-electrode system. 5 mM $K_4[Fe(CN)_6]/K_3[Fe(CN)_6]$ (1:1) was employed as redox couple in aqueous solution for electrochemical characterization. The scanning rate of CV was fixed at 0.02 V/s and the transmission spectrum was simultaneously recorded and saved every 5 s. Thus, the transmission spectrum was obtained to represent optical LSPR, in 0.1 V steps during voltage scanning with different electrochemical current (Fig. 7c). Figure 8 shows a photograph of the electrochemical LSPR measurement apparatus. For optical detection, there were three fiber bundles, two collimating lenses, an optical fiber attenuator, a light source and a spectrophotometer. Fiber bundles were used to provide optical linkage between the lens, the attenuator, the light source, and the spectrophotometer. The spectrophotometer was also directly connected to the light source by data cable. Thus, the spectrophotometer can synchronously capture light emitted by the light source and delivered through nanoCA devices. For electrochemical detection, the nanoCA device was used as the working electrode, while platinum and Ag/AgCl electrodes were used as counter electrode and reference electrodes, respectively. These three electrodes were all linked to an

electrochemical workstation and inserted into a spectrometer measuring cell filled with redox solution. Careful arrangement of these three electrodes should maintain successful delivery through the cell.

- The electrochemical LSPR measurements for nanoCA were further carried out and analyzed with transmission spectrum and synchronous CV scanning. As seen in Fig. 7b, a significant LSPR dip shift was recorded in the transmission spectrum when electrochemical current on the nanoCA surface was changed from 0 to 0.2 mA. The resonance wavelength was shifted from 558 to 564 nm but there was no significant shift observed for LSPR peaks.
- Optical measurements within CV scanning were carried out and the wavelength shifts of LSPR dips were shown in Fig. 7c. During scanning, the wavelength of dip was shifted from 566 nm to 573 nm with an increase of current from 0.25 to 0.5 mA. When the current returned to 0.25 mA, the wavelength also decreased with declining current. These results indicate that the current change on the nanoCA surface can modulate LSPR of nanoCA and produce a wavelength shift in LSPR. The LSPR in transmission dip around 550 nm can be enhanced by electrochemical current and can be analyzed as an indicator in electrochemical LSPR detecting.

3.6.2 Electrochemical LSPR Spectroscopy as Biosensor for Immunoreaction

Utilizing electrochemical enhancement for LSPR on nanoCA, electrochemical LSPR biosensors can be fabricated with higher sensitivity in the synchronous measurement mode. Many biointeractions such as immunoreaction can be probed by electrochemical LSPR spectroscopy on the nanoCA.

- The nanoCA was modified by anti-BSA which can specifically bind to BSA by self-assembly (for methods *see* Subheading 3.4).
- One milliliter BSA solutions at different concentrations can be added in wells of the 96-well plates by pipette.
- The CV scanning can be performed on the nanoCA device (*see* Subheading 3.6). The redox current can be generated from the redox couple and modulated by the binding of BSA to anti-BSA. The CV scanning can provide redox currents around 0.1 and 0.3 V in the voltammogram with electrochemical reactions.
- The transmission spectrum was recorded when CV scanning reached 0.3 V (Fig. 9a, *see* Subheading 3.6). LSPR dip shifts were elicited by the conjunction of anti-BSA and BSA on the surface of nanoCA and enhanced by the CV scanning from 9 to 15 nm. Due to the redox current, the negative protein of HSA also elicited a wavelength shift of about 3 nm. However, this was much lower than the response to BSA of about 15 nm with

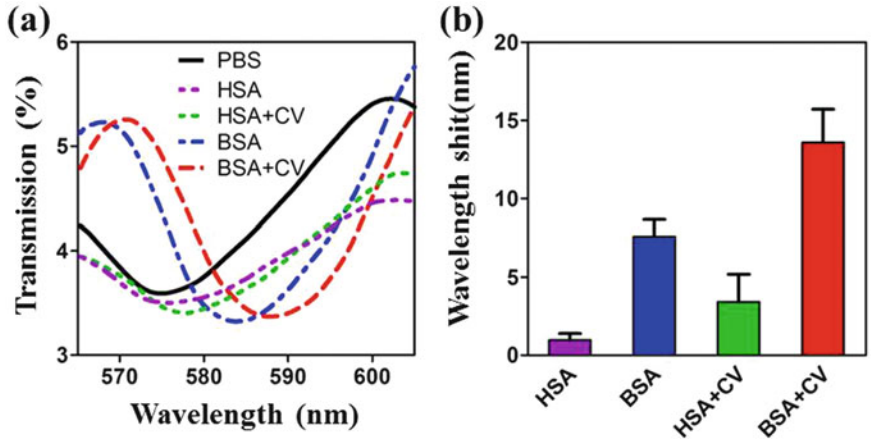

Fig. 9 Electrochemical LSPR detection for specific binding of proteins. (**a**) The transmission spectrum of nanoCA with PBS, 100 μg/ml BSA and BSA plus synchronous CV scanning, 100 μg/ml HAS and HSA plus CV scanning. (**b**) Statistic for shifts in dip wavelength of HSA, HSA plus CV, BSA and BSA plus CV (mean ± SD, $n = 6$)

electrochemical enhancement (Fig. 9b). These results suggest that the electrochemically coupled LSPR measurement had redox currents that modulate LSPR dip shift, in addition to that resulting from RI change. In fact, LSPR measurement with and without CV had detection limits of 13 and 25 μg/ml, respectively, for BSA detection. Thus, the electrochemically enhanced biosensor fabricated with electrochemical LSPR had higher response and sensitivity than that of conventional optical methods.

3.6.3 Electrochemical LSPR Spectroscopy as Biosensor for Enzymatic Activity

The electrochemical LSPR spectroscopy can also be used in thrombin detection [28]. The detection can be performed by the following steps.

- As shown in Fig. 10a, polyethylene glycol (PEG), peptide (CLVPRGSC), and bovine serum albumin (BSA) were immobilized on surface of nanoCA with the self-assembly (methods, *see* Subheading 3.4), while peptides were used as probes for thrombin.
- One milliliter thrombin solutions at different concentrations can be added in wells by pipette. Thrombin can cleave specific sites of peptide sequences and remove BSA from the surface of nanoCA, thereby modulating LSPR transmission spectra.
- Spectrographic measurement was coupled with electrochemical voltage at 3 V to dissociative BSA from the nanoCA surface and increase LSPR wavelength shift responses. The measurement apparatus was the same as described above (*see* Subheading 3.6).

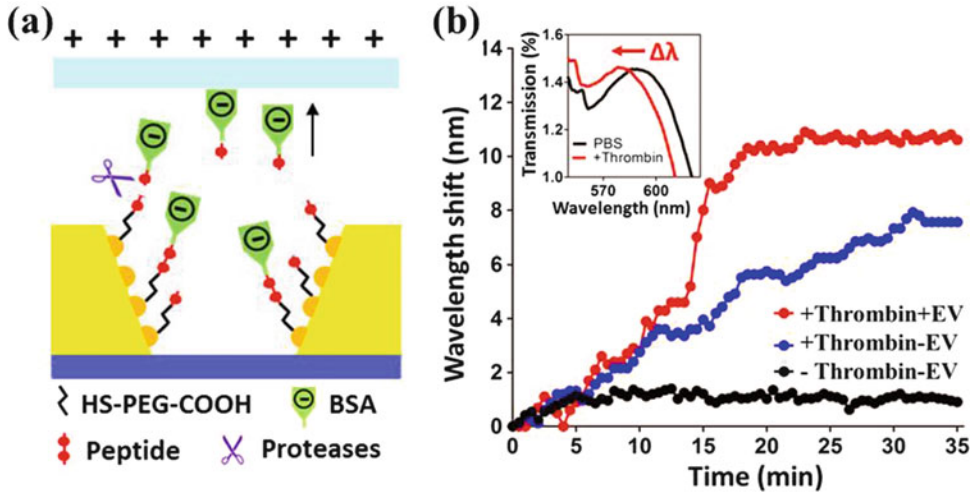

Fig. 10 Electrochemical LSPR sensor for thrombin detection. (**a**) Design of electrochemical LSPR sensor for thrombin using self-immobilization of protein on nanoCA. (**b**) LSPR responses of wavelength shifts of the nanoCA for thrombin detections with (+) and without (−) electrochemical enhancement, electrochemical voltage (EV)

The results for thrombin detection are shown in Fig. 10b. The presence of thrombin can selectively catalyze cleavages at Arg-Gly bonds of peptides, remove BSA from the nanoCA sidewall, and generate time-dependent shifts in resonance wavelength of nanoCA (*see* **Notes 10** and **11**).

– The transmission spectrum can be analyzed by LSPR wavelength shifts with electrochemical enhancement. As expected, as the electrochemical voltage is increased LSPR wavelength shifts significantly. There was stronger voltage enhancement in the presence of thrombin at high concentrations. Indeed, the electrochemically enhanced LSPR biosensor had higher sensitivity and shorter response time than the sensor utilizing LSPR alone. This provides a promising approach for designing more sensitive and rapid LSPR sensors.

4 Notes

1. Phosphate buffer saline (PBS) was used as the solvent for proteins. The solution was prepared by dissolving 137 mM NaCl, 2.68 mM KCl, 1.47 mM KH_2PO_4, and 8.10 mM Na_2HPO_4 in pure water and pH was fixed at 7.4.
2. 2-(morpholino)ethanesulfonic acid (MES) buffer was used as buffer solution for protein self-immobilization. It was prepared by dissolving 100 mM MES and 500 mM NaCl, and its pH was fixed at 6.0.

3. 1-ethyl-3-(3-dimethylaminopropyl) carbodiimide (EDC) solution was prepared at 2 mM, while MES buffer was used as the solvent.
4. *N*-hydroxy-succinimide (NHS) solution was prepared at 5 mM, while MES buffer was used as the solvent.
5. Carboxy-poly(ethylene)-thiol (HOOC-PEG-SH, 2 kDa) was used as linkage between proteins and nanoCA device. The solution was prepared at 1 mg/ml, while ethyl alcohol and pure water with rate 7:3 were used as solvent of HOOC-PEG-SH.
6. OBPs, Acer-ASP2, were cloned from the full-length cDNA of adult worker bees, *Apis cerana* cerana. The protein was resuspended in PBS solution at 500 μg/ml and stored at 4 °C for biosensor experiments (*see* **Note 1**).
7. Peptides used in our study were synthesized by the standard solid phase method. Synthesized peptides were tested by high-performance liquid chromatography (HPLC) and mass spectrometry (MS) to verify amino acid sequence and purity. The peptides were stored in the form of freeze-dried powders before experiments and dissolved in PBS at 500 μg/ml.
8. The proteins involved in the study, such as OBPs, peptides, and BSA, should all be dissolved in PBS solution for use during experiments. Before experiments, proteins should be stored at 4 °C to maintain bio-activity.
9. In designing the electrochemical LSPR biosensor for thrombin, the protein immobilization on nanoCA was completed by two steps of self-assembly of the peptide and BSA. The steps are both as described for linking proteins to HS–PEG–COOH in the above Method section.
10. Protein immobilization on nanoCA should be tested to verify efficient combination of protein and the nanoCA device. Generally, electrochemical impedance spectroscopy and optical spectroscopy can be used to verify the combination.
11. In the electrochemical LSPR detection for thrombin, the electrochemical voltage can range from 0.1 to 5 V. The voltage at 3 V used in our study was optimized to obtain better sensitivity and shorter sensor response times.

Acknowledgments

This work was supported by the National Natural Science Foundation of China (Grant No. 81371643), the Zhejiang Provincial Natural Science Foundation of China (Grant No. LR13H180002).

References

1. Homola J (2008) Surface plasmon resonance sensors for detection of chemical and biological species. Chem Rev 108:462–493
2. Vollmer F, Arnold S (2008) Whispering-gallery-mode biosensing: label-free detection down to single molecules. Nat Methods 5:591–596
3. Nair RV, Vijaya R (2010) Photonic crystal sensors: an overview. Prog Quant Electron 34:89–134
4. Saha K, Agasti SS, Kim C et al (2012) Gold nanoparticles in chemical and biological sensing. Chem Rev 112:2739–2779
5. Willets KA, Van Duyne RP (2007) Localized surface plasmon resonance spectroscopy and sensing. Annu Rev Phys Chem 58:267–297
6. Mayer KM, Hafner JH (2011) Localized surface plasmon resonance sensors. Chem Rev 111:3828–3857
7. Gao HW, Henzie J, Odom TW (2006) Direct evidence for surface plasmon-mediated enhanced light transmission through metallic nanohole arrays. Nano Lett 6:2104–2108
8. Anker JN, Hall WP, Lyandres O et al (2008) Biosensing with plasmonic nanosensors. Nat Mater 7:442–453
9. Stewart ME, Anderton CR, Thompson LB et al (2008) Nanostructured plasmonic sensors. Chem Rev 108:494–521
10. Cao J, Sun T, Grattan KT (2014) Gold nanorod-based localized surface plasmon resonance biosensors: a review. Sens Actuators B 195:332–351
11. Cheng XR, Wallace GQ, Lagugné-Labarthet F et al (2015) Au nanostructured surfaces for electrochemical and localized surface plasmon resonance-based monitoring of α-synuclein–small molecule interactions. ACS Appl Mater Interfaces 7:4081–4088
12. Boltasseva A (2009) Plasmonic components fabrication via nanoimprint. J Opt A Pure Appl Opt 11:114001
13. Pimpin A, Srituravanich W (2011) Review on micro-and nanolithography techniques and their applications. Eng J 16:37–56
14. Zhang D, Lu Y, Jiang J et al (2015) Nanoplasmonic biosensor: coupling electrochemistry to localized surface plasmon resonance spectroscopy on nanocup arrays. Biosens Bioelectron 67:237–242
15. Zhang D, Lu Y, Zhang Q et al (2015) Nanoplasmonic monitoring of odorants binding to olfactory proteins from honeybee as biosensor for chemical detection. Sensor Actuat B Chem 221:341–349
16. Zhang D, Zhang Q, Lu Y, et al. (2016) Peptide functionalized nanoplasmonic sensor for explosive detection. Nano-Micro Lett 8:36–43
17. Gartia MR, Hsiao A, Pokhriyal A et al (2013) Colorimetric plasmon resonance imaging using nano lycurgus cup arrays. Adv Opt Mater 1:68–76
18. Stewart ME, Mack NH, Malyarchuk V et al (2006) Quantitative multispectral biosensing and 1D imaging using quasi-3D plasmonic crystals. Proc Natl Acad Sci U S A 103:17143–17148
19. Kuznetsov AI, Evlyukhin AB, Goncalves MR et al (2011) Laser fabrication of large-scale nanoparticle arrays for sensing applications. ACS Nano 5:4843–4849
20. Kee JS, Lim SY, Perera AP et al (2013) Plasmonic nanohole arrays for monitoring growth of bacteria and antibiotic susceptibility test. Sensor Actuat B Chem 182:576–583
21. Lu Y, Li H, Zhuang S et al (2014) Olfactory biosensor using odorant-binding proteins from honeybee: Ligands of floral odors and pheromones detection by electrochemical impedance. Sensor Actuat B Chem 193:420–427
22. Lu Y, Yao Y, Zhang Q et al (2015) Olfactory biosensor for insect semiochemicals analysis by impedance sensing of odorant-binding proteins on interdigitated electrodes. Biosens Bioelectron 67:662–669
23. Li H-L, Zhang Y-L, Gao Q-K et al (2008) Molecular identification of cDNA, immunolocalization, and expression of a putative odorant-binding protein from an Asian honey bee, *Apis cerana* cerana. J Chem Ecol 34:1593–1601
24. Jaworski JW, Raorane D, Huh JH et al (2008) Evolutionary screening of biomimetic coatings for selective detection of explosives. Langmuir 24:4938–4943
25. Smith RG, D'Souza N, Nicklin S (2008) A review of biosensors and biologically-inspired systems for explosives detection. Analyst 133:571–584
26. Ramoni R, Bellucci S, Grycznyski I et al (2007) The protein scaffold of the lipocalin odorant-binding protein is suitable for the design of new biosensors for the detection of explosive components. J Phys Condens Matter 19:395012

27. Kuang Z, Kim SN, Crookes-Goodson WJ et al (2009) Biomimetic chemosensor: designing peptide recognition elements for surface functionalization of carbon nanotube field effect transistors. ACS Nano 4:452–458

28. Zhang D, Zhang Q, Lu Y et al (2015) Electrophoresis-enhanced nanoplasmonic biosensor with nanocup arrays for protease detection in point-of-care diagnostics. China Nanomed 2015:202